

Three-Parameter Formula for the Electronic Stopping Cross Section at Nonrelativistic Velocities*

David K. Brice

Sandia Laboratories, Albuquerque, New Mexico 87115

(Received 12 June 1972)

The Firsov formalism for calculating the electronic stopping cross section has been modified by (i) giving a precise quantum-mechanical definition of the electron flux across the Firsov plane in terms of the bound-state wave functions and (ii) by including the relative motion of the Firsov plane in the flux calculation. This formalism is then extended in a semiphenomenological manner to the velocity region where the relative velocity of the colliding atoms is of the same order of magnitude as the orbital velocities of their electrons. When hydrogenic $1s$ wave functions are used, three adjustable parameters result from this treatment, one from the modification of the Firsov formalism and two from the extension to higher velocities. It is found that adjustment of these parameters to give a best fit to experimental data yields an expression which accurately gives the electronic stopping cross section S_e for any collision partners, and at all nonrelativistic velocities. The three parameters are considered as adjustable for the purposes of this paper, but it is shown here that the low-energy parameter Z is calculable from first principles. In addition, one of the high-energy parameters a is shown to be a linear function of the target atomic "radius."

I. INTRODUCTION

In this paper a formula is presented for the electronic (inelastic) stopping cross section S_e for atomic projectiles penetrating material targets.¹ The formula was originally developed to improve agreement between experiment and theory at relatively low collision velocities between $1s$ electron atoms. It has been found, however, that the formula accurately represents S_e for collisions between projectiles and targets having other than $1s$ electrons and at all nonrelativistic velocities. The formula contains three parameters which are adjusted to give a best fit between experiment and theory. In general one finds that for those cases in which various different experiments are in good agreement the formula can be fit to experiment with a root-mean-square percentage error of ~ 1 – 2% over the energy (velocity) range 0 – 10 MeV/amu. A brief review of the current status of the theory² of S_e will illustrate the usefulness of such a formula.

Theorists usually recognize three velocity regimes for such calculations: (i) a high-velocity regime for which the projectile velocity u is much greater than the orbital velocities $\{v_i\}$ of the atomic electrons of both the incident atom and the target, (ii) an intermediate-velocity regime for which u is the same order of magnitude as some of the $\{v_i\}$, and (iii) a low-velocity regime for which u is much smaller than all the $\{v_i\}$. Binary atomic collisions are usually assumed in all three regimes.

In the high-velocity regime the incident atom is stripped of all its electrons as it penetrates the target, and the Bethe-Bloch theory³ with corrections^{4,5} is applicable. This approach generally gives agreement between theory and experiment

$\sim 1\%$ except in the few MeV/amu region for the heavier atomic projectiles.⁵ In the low-velocity regime, the incident atom is assumed to retain all its electrons, and approaches such as those of Lindhard *et al.*,⁶ and Firsov^{7–11} have been reasonably successful. Agreement between experiment and theory is generally within ~ 20 – 30% in this regime, although agreement can be improved to within ~ 4 – 7% if certain parameters of the theory are considered as adjustable (see below). In the intermediate-velocity regime, the calculations are considerably more complicated since one can use neither an impulse (high-velocity) nor an adiabatic (low-velocity) approximation. Further, in this regime the average charge state of the projectile depends on its energy, as well as the target material. Corrections to the Bethe-Bloch theory for simple atomic systems (e.g., those of Hirshfelder and Magee¹²) lead to reasonable agreement ($\sim 10\%$) with experiment in this regime, but such calculations are prohibitively difficult for more complicated atomic structures. At present there is no basic theoretical treatment which adequately treats this velocity regime, and only semiphenomenological treatments^{2,13,14} are available.¹⁵

In all three regimes, because of the complexity of atomic structure for all except the simplest of systems, certain properties of the colliding atoms must be regarded as adjustable parameters to be determined through experiment. In the high-velocity regime the mean-excitation potential⁵ I_{adj} must be determined in this fashion. The low-velocity-regime theory^{8–11} predicts $S_e = ku$. Experiment shows that $S_e = ku^p$ in this region with p a slowly varying function of u with value close to unity. Although theoretical expressions for k are avail-

able,^{6,7} they are often incorrect by $\sim 20\text{--}30\%$, and k and p are usually determined by a fit to experimental measurements. With k and p so adjusted, agreement with experiment is $\sim 4\text{--}7\%$.¹⁶ In the intermediate-velocity regime there are a variety of adjustable parameters which must be determined depending on the particular approach used. Among the adjustable parameters are the effective charge of the incident ion (a velocity-dependent parameter),¹⁷ and the shell corrections C/Z which are necessary when the projectile velocity u is of the order of the atomic electron velocities.¹³ With proper adjustment of these several parameters, agreement with experiment is generally better than $\sim 8\%$ in the intermediate-velocity regime.

In summary the three-velocity-regime approach requires ~ 5 or more adjustable parameters to adequately explain the experimentally observed values of S_e , and over-all accuracies from 1 to 8% are obtained. Curves of S_e for projectiles, or for targets, for which there are no experimental measurements can be obtained in this approach by noting the regular progression of the various parameters with projectile atomic number (Z_1) or mass (A_1), or with a target atomic number (Z_2) or mass (A_2), and then extrapolating the parameters to the case of interest. Since each of the three velocity regimes is treated relatively independently of the others, however, there is usually no accurate way of extrapolating results from one velocity regime into another.

The semiphenomenological treatment of Northcliffe and Schilling¹⁴ (NS) should also be mentioned, although their approach does not utilize directly the three velocity regimes discussed above. Recognizing the general similarity in electronic stopping power curves, they assume, as a first approximation, that the *relative* stopping power of two target materials is independent of projectile identity at a given projectile velocity. Thus, a set of stopping cross sections for some particular target material (chosen as Al by NS) and a set of *relative* stopping cross sections for other target materials would allow one to construct the stopping cross-section curve for any projectile-target combination. Their set of curves thus constructed is reasonably successful in giving stopping cross sections over all three velocity regimes with typical errors being $\sim 10\text{--}15\%$. In certain cases, however, errors $\sim 50\text{--}100\%$ or more are found, particularly at the lower incident atom velocities (~ 0.1 MeV/amu) or for the lighter atomic projectiles. The problem of extrapolation from one velocity regime to another is clearly overcome by the NS treatment; however the reduction in accuracy accompanying their approach often negates this virtue.

From this discussion, it is clear that the formula with three adjustable parameters, which is pre-

sented in this paper and which accurately gives S_e in all three velocity regimes, is a distinct improvement over the present descriptions of the stopping cross section. Among the advantages of such a formula are (i) a formula with only three adjustable parameters which is *more accurate* in the low- and intermediate-velocity regimes *than any other approach*, (ii) a smooth curve which allows a determination of S_e in velocity regions for which there are no experimental measurements, and (iii) a set of parameters which can be extrapolated to projectile-target combinations for which there are no measurements to allow S_e determinations for these cases. This list should not be considered as exhaustive since other advantages could also be mentioned such as the ease of determining S_e by merely entering the independent variable (velocity, energy) in a single simple analytic formula.

As mentioned earlier, the formula was derived in calculations which were originally intended to improve the agreement between theory and experiment in the low-velocity, and the lower part of the intermediate-velocity regimes. The fundamental physical assumptions which have gone into the calculations are thus those appropriate to this velocity region, and by and large, classical concepts are utilized. The basic physical arguments given are relatively crude, and most certainly not correct in the high-velocity regime. Nevertheless, the formula which results from the treatment is in excellent agreement with experiment and previous theory over *all three* velocity regimes. While the "derivation" must thus be regarded as a prescription for determining S_e , rather than a development from fundamental principles, the resultant formula unifies stopping cross-section formulas over all three velocity regimes with a reduction in the net number of adjustable parameters.

The derivation of the formula is based on a modification and an extension of the low-energy approach of Firsov.⁷ A brief discussion of the Firsov theory and a derivation of the three-parameter formula are given in Sec. II of this paper. Also included in Sec. II is a brief discussion of the parameters in the formula. In Sec. III the formula is compared with the predictions of several other theoretical approaches for hydrogen incident on hydrogen and helium incident on helium. Determination of the three parameters for hydrogen, helium, and sulfur atoms incident on a variety of gaseous targets is presented in Sec. IV, and discussion and conclusions are presented in Sec. V.

II. FORMULA

A. Firsov Theory

In the Firsov theory⁷ a plane, which perpendicularly bisects the line of centers of two colliding

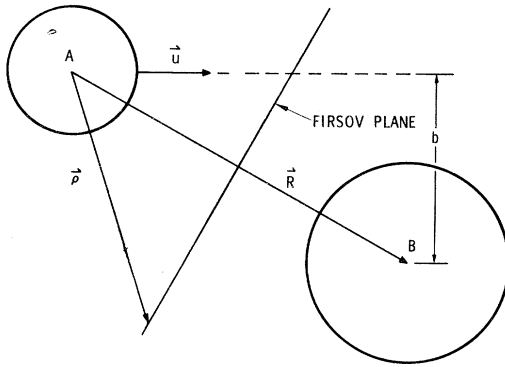


FIG. 1. Geometry for calculations using the Firsov theory. The relative position vector \vec{R} is bisected by and is normal to the Firsov plane. The origin of the z axis is at atom A which is shown incident on atom B with relative velocity \vec{u} and impact parameter b . The vector $\vec{\rho}$ locates a point on the Firsov plane relative to the center of atom A .

atoms, is regarded as dividing space into two distinct physical regions as illustrated in Fig. 1. All of the electrons on a given side of the plane are regarded as belonging to the atom on that side of the plane, and have the same average velocity. When an electron crosses the plane it changes its atomic identification and transfers momentum $\pm m\vec{u}$ to the recipient atom. Here m is the rest mass of an electron, and \vec{u} is the relative velocity of the colliding atoms. The total flux of electrons across the plane in one direction, multiplied by $\pm m\vec{u}$, represents a force on the recipient atom resulting in an energy exchange. Integration of this energy exchange over impact parameters b and summing over both atoms then gives the electronic stopping cross section S_e .

Referring to Fig. 1, let Φ_{AB} be the flux of electrons from atom A to atom B across the Firsov plane. The force on atom B , \vec{F}_B , due to this electron flux is then given by

$$\vec{F}_B = \Phi_{AB} m \vec{u}. \quad (1)$$

The work done on atom B by this force dW_B as the atom moves a distance $d\vec{R}_B$ is then

$$dW_B = \Phi_{AB} m \vec{u} \cdot d\vec{R}_B. \quad (2)$$

Similarly, the work done on atom A by the electron flux across the plane from atom B to atom A , Φ_{BA} , is given by dW_A , where

$$dW_A = -\Phi_{BA} m \vec{u} \cdot d\vec{R}_A \quad (3)$$

and $d\vec{R}_A$ is the distance moved by atom A .

The minus sign on Eq. (3) arises because the electrons crossing the plane from B to A originally have an average velocity $-\vec{u}$ relative to A . The total work done on the system by forces due to the electron flux across the Firsov plane is then dW

$$= dW_A + dW_B.$$

Firsov assumes that $\Phi_{AB} = \Phi_{BA} = \Phi$, and thus

$$\begin{aligned} dW &= \Phi m \vec{u} \cdot (d\vec{R}_B - d\vec{R}_A) \\ &= \Phi m \vec{u} \cdot d\vec{R}, \end{aligned} \quad (4)$$

where \vec{R} is the relative coordinate from atom A to atom B . Firsov further assumes that the paths of the colliding atoms are rectilinear and that the relative velocity \vec{u} is constant throughout the collision. The total work done by the electron flux during the collision is then $W(b)$, where b is the impact parameter for the collision, and

$$W(b) = -m u \int_{-\infty}^{\infty} \Phi dx'. \quad (5)$$

The variable x' in Eq. (5) is the negative of the projection of \vec{R} onto the direction of relative velocity \vec{u} .

Firsov identifies $W(b)$ as the inelastic energy loss of the collision. The stopping cross section S_e can be obtained from $W(b)$ through the definition

$$S_e = 2\pi \int_0^{\infty} W(b) b db. \quad (6)$$

The essential feature in calculating S_e through the Firsov approach is the determination of the flux across the Firsov plane. Once that has been accomplished one merely evaluates Eqs. (5) and (6) using the determined flux. Firsov evaluates the electron flux across the plane in a semiclassical fashion by assuming a spherical distribution of electron velocities at every point in space. The flux $d\Phi$ across an element of area dA at some point on the Firsov plane is then given by $d\Phi = \frac{1}{4} n v dA$, where n and v are, respectively, the electronic density and the average speed of the electrons at the point of interest on the plane. Firsov evaluates n and v using a Thomas-Fermi model of the colliding atoms. The total flux Φ is then obtained by integration over the Firsov plane. Modifications to the Firsov theory have been presented by Bhalla *et al.*,⁹ Cheshire *et al.*,¹⁰ and Wilson *et al.*¹¹ Although other refinements to the theory are considered by these three groups, the evaluation of the flux is carried out in essentially the fashion outlined above with the exception that more realistic estimates of the electronic density n and average speed v are utilized.

A semiclassical flux determination for the Firsov calculation is necessary since the quantum-mechanical formalism gives a flux of identically zero when bound-state wave functions are used. This occurs because the flux in both directions across the plane is included in the total. In this paper, however, a precise quantum-mechanical definition of the flux is made possible by defining a "partial" bound-state wave function which contains only that portion of the electronic motion which will contribute to the flux in one direction

across the plane. The resultant definition of flux also takes into account the relative motion of the colliding atoms, which in effect amounts to a relative motion of each atom with respect to the Firsov plane.

B. Flux

Let $\psi(\vec{r})$ be a one-electron bound-state wave function, where \vec{r} locates the electron relative to the center of mass of the atom to which it belongs. Let $\varphi(\vec{k})$ be the corresponding wave function in momentum space. These two functions are Fourier transforms of each other with the appropriate integrals being defined over all \vec{k} , \vec{r} space. Thus for $\vec{r} = (x, y, z)$, $\vec{k} = (k_x, k_y, k_z)$,

$$\varphi(\vec{k}) = (1/2\pi)^{3/2} \int_{-\infty}^{\infty} dx \int_{-\infty}^{\infty} dy \int_{-\infty}^{\infty} dz e^{-i\vec{k}\cdot\vec{r}} \psi(\vec{r}) \quad (7a)$$

and

$$\psi(\vec{r}) = (1/2\pi)^{3/2} \int_{-\infty}^{\infty} dk_x \int_{-\infty}^{\infty} dk_y \int_{-\infty}^{\infty} dk_z e^{i\vec{k}\cdot\vec{r}} \varphi(\vec{k}) dk_z \quad (7b)$$

At some instant let the two colliding atoms be arrayed as indicated in Fig. 1, and let the z axis of the coordinate system be chosen as parallel to \vec{R} . The origin of the coordinate system is chosen at the center of mass of one of the atoms, for example, atom A . The Firsov plane is thus perpendicular to the z axis of the coordinate system and at a distance $\frac{1}{2}R$ from the origin ($R = |\vec{R}|$). Let $\vec{\rho}$ locate a point on the Firsov plane relative to A and let the plane be moving relative to atom A with a velocity $\vec{w} = (w_x, w_y, w_z)$ at that point. (The motion of the plane relative to the two atoms is due to the relative motion of the atoms themselves.)

A "partial" wave function $\psi_+(\vec{\rho})$ is now defined as

$$\psi_+(\vec{\rho}) = (1/2\pi)^{3/2} \int_{-\infty}^{\infty} dk_x \int_{-\infty}^{\infty} dk_y \int_{k_0}^{\infty} dk_z e^{i\vec{k}\cdot\vec{\rho}} \varphi(\vec{k}) dk_z, \quad (8)$$

with $k_0 = mw_z/\hbar$. The wave function $\psi_+(\vec{\rho})$ thus contains only those plane waves which are traveling from the A side of the plane to the B side, and which have sufficient velocity to overtake and cross the plane. The flux of electrons from the A side to the B side of the plane can then be evaluated with the usual quantum-mechanical formalism through

$$\Phi = \int \left[\frac{\hbar}{2im} \left(\psi_+^* \frac{\partial \psi_+}{\partial z} - \psi_+ \frac{\partial \psi_+^*}{\partial z} \right) - \frac{\hbar k_0}{m} |\psi_+|^2 \right] dA. \quad (9)$$

The first two terms in the integrand in (9) represent the usual calculation of the flux across a stationary plane using the wave function ψ_+ . The last term in the integrand is a correction to the first two arising from the motion of the plane. The integration in (9) is over the Firsov plane.

In defining the flux as above, the spirit of the Firsov approach has been retained. Plane waves

traveling in the "wrong" direction at the point $\vec{\rho}$ have been eliminated from the wave function since they represent electrons traveling from the B side of the plane to the A side. According to the Firsov approach, such electrons "belong" to the B atom, and that flux should be calculated using the appropriate wave function for the B atom. Also eliminated from the wave function are those plane waves which while traveling in the proper direction lack sufficient velocity to overtake and cross the plane.

When the hydrogenic $1s$ wave function is used in Eqs. (8) and (9), and the resultant flux is entered in Eqs. (5) and (6), one finds a one-electron contribution S'_e to the electronic stopping cross section (see Appendix A), where

$$S'_e = \frac{4\hbar^2}{5m} \left[\epsilon^{1/2} \left(\frac{30\epsilon^3 + 83\epsilon^2 + 74\epsilon + 21}{3(1+\epsilon)^3} \right) + (10\epsilon + 1) \arctan \epsilon^{1/2} \right]. \quad (10)$$

In (10) $\epsilon \equiv (u/2v_0Z)^2$, where v_0 is the Bohr velocity e^2/\hbar and Z is the effective nuclear charge.¹⁸ The translatory motion of the Firsov plane (parallel to the z axis) has been included in (10), but not the rotational motion. Inclusion of the rotational motion leads to a nonphysical singularity for small impact parameters, and therefore it was not included. The electronic stopping cross section is obtained, in the present modification of Firsov theory, by summing (10) over all the electrons of the two colliding atoms. This expression is expected to be valid over a velocity region for which the basic assumptions of the Firsov approach are valid.

If the colliding atoms interact significantly over a distance l during the collision, the Firsov approach requires that during a time $\tau (=l/u)$, (i) a given electron must have sufficient time to cross the Firsov plane, (ii) it must find electrons of the recipient atom in the region near the Firsov plane with which to interact, and (iii) enough energy must be exchanged between the interacting electrons to cause the crossing electron to become associated with the recipient atom. From a classical point of view, at small τ , conditions (i) and (ii) will each have probability of occurrence proportional to τ/T , where T is the average orbital period of the atomic electrons. That is, for short collision times the probability of finding an electron on any given part of its orbit during the collision is proportional to τ/T . Further, if one takes the probability of condition (iii) as proportional to the energy exchange, then at small τ an impulse approximation yields probability proportional to τ^2 . These arguments suggest that S'_e of Eq. (10) should be reduced by a factor proportional to τ^n at small τ with $n \sim 4$.

An invented function which has appropriate large

and small τ behavior is $[1 + (T/\tau)^n]^{-1}$. In terms of relative velocity this function is $f(u)$, where

$$f(u) = [1 + (au/v_0)^n]^{-1}. \quad (11)$$

In Eq. (11) the parameter a is given by $a = v_0 T/l$. Since $v_0 T$ and l each represent lengths of atomic dimensions it is expected that $a \sim 1$.

The stopping cross section S_e is obtained by multiplying S'_e by $f(u)$, and then summing over all electrons on the two colliding atoms. Thus, if Z_1 and Z_2 are the atomic numbers of the projectile and target, respectively,

$$S_e(u) = (Z_1 + Z_2) S'_e(u) f(u). \quad (12)$$

The parameters a and n appearing in $f(u)$ and the parameter Z which appears in $S'_e(u)$ are considered as adjustable parameters to be determined by experiment.

Some general observations on the low- and high-velocity behavior of the formula in Eq. (12) can be obtained from an examination of Eqs. (10) and (11), respectively. From Eq. (10) it is easily verified that the slope of $\ln S'_e$ vs $\ln u$ increases monotonically from 1 at low velocities to 2 at high velocities. Similarly, from Eq. (11) one sees that the slope of $\ln f$ vs $\ln u$ decreases monotonically from zero at low velocities to $-n$ at high velocities. Thus, at low velocities $\ln S_e$ vs $\ln u$ will have a slope which is a slowly varying function of u , with a value near 1. This is in agreement with the experimentally observed behavior of S_e .¹⁶ Whether the function is superlinear or sublinear at a particular velocity will depend on whether S'_e or f has the dominating effect on the change in slope at that velocity, which in turn will depend on the values of the parameters a , n , and Z . In the high-velocity limit S_e will vary as u^{2-n} . Since it has previously been argued that $n \sim 4$ the stopping cross section will vary in this limit inversely with u to a power ~ 2 . The nonrelativistic Bethe-Bloch formula³ predicts that S_e will vary as $u^{-2} \times \ln \alpha u$ in this region with α a constant. Although the formula given here is not identical with that of Bethe-Bloch, a power-law approximation could be expected to be relatively accurate because of the slow variation of $\ln \alpha u$ with u . Such behavior is exhibited explicitly in the curves of Fig. 2 of Ref. 14, particularly for those ions for which the maximum S_e value occurs at an energy well below the relativistic limit.

The parameter Z appears only in the expression for S'_e and therefore is determined by the low-velocity behavior of S_e since $f(u) \sim 1$ in this region. For purposes of estimating Z values later it will be useful to note that the low-velocity limit of S_e will be given by

$$S_e \rightarrow [(Z_1 + Z_2)(16\hbar^2)/(5mv_0Z)]u. \quad (13)$$

The two parameters a and n occur in that part of $f(u)$ which is important at high velocities, and are therefore most sensitive to the high-velocity behavior of S_e . In previous modifications of the Firsov theory⁹⁻¹¹ the low-velocity behavior of S_e has been calculated from first principles with results which are in agreement within $\sim 10\%$ with experiment. With the flux definition given in Eqs. (8) and (9) of this paper the agreement of such calculations with experiment should be improved. Thus, in principle, one has a method of calculating Z from first principles.

We will show later in this paper that the parameter a correlates well with certain properties of the target atoms for a fixed incident ion. With a so determined and Z evaluated as indicated above, the final parameter n can then be evaluated from a single high-energy measurement, or from the Bethe-Bloch formula.³ Thus, while all three parameters are considered as adjustable in this paper, one, and perhaps two of them, appear to be determinable from first-principles calculations.

III. 1s ELECTRON PROJECTILES AND TARGETS

The formula presented in Sec. II for the electronic stopping cross section S_e has been derived using 1s hydrogenic wave functions. Since hydrogen and helium atoms have only 1s electrons in their ground states, a comparison of the formula with experiments which utilize these two atoms as projectiles and targets offers an opportunity to test the theory against experiment. In addition, such comparison will show the improved accuracy of the present formula over other theoretical approaches. In particular, the case of hydrogen incident on hydrogen should prove quite illustrative since the remarks above concerning a first-principles calculation of Z are pertinent. That is, we know that $Z=1$ for this case, and only the parameters a and n remain to be determined.

Figure 2 shows the energy dependence of S_e for hydrogen incident on hydrogen gas over the energy interval 0-7 MeV. The experimental points shown there are from the tabulation by Bichel¹³ and the experimental results of Phillips¹⁹ and Reynolds *et al.*²⁰ The theoretical curves are from the Bethe-Bloch theory³ (with $I_{adj} = 19$ eV, labeled BB), the Bethe-Bloch theory with corrections as calculated by Hirshfelder and Magee¹² (HM), and the low-energy theories of Lindhard *et al.*⁶ (LSS), Firsov^{7,8} (F), and Bhalla *et al.*⁹ (BH) as well as the results of the present calculation (BR). The parameters a and n have been determined by a least-squares error fit of Eq. (12) to experiment using $Z=1$. Values which result are $a=0.660$ and $n=3.60$. It is seen in Fig. 2 that the present approach gives quite good agreement between experiment and theory over an astonishing range of en-

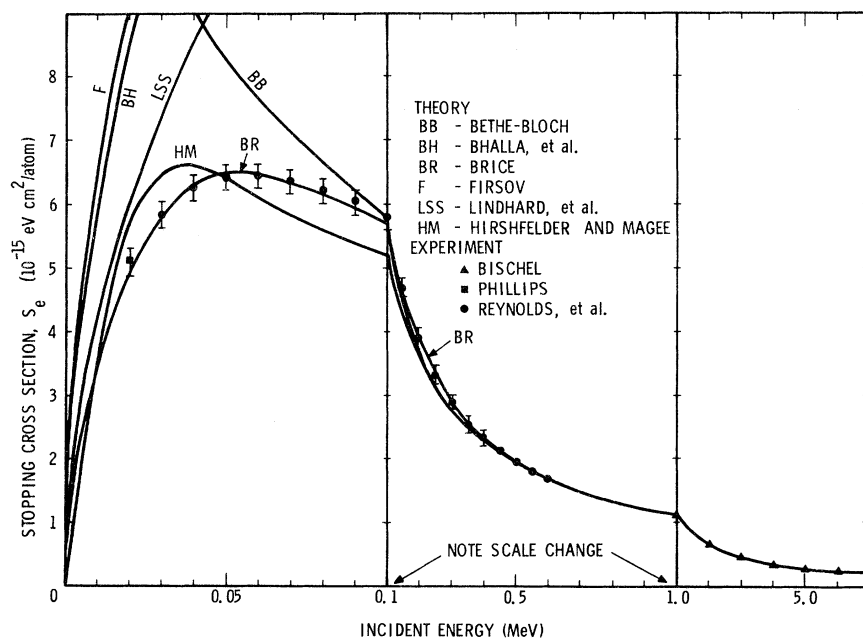


FIG. 2. Electronic stopping cross section vs incident energy for hydrogen incident on hydrogen. The theoretical curves shown are from the present paper and Refs. 5-7, 9, and 12. The experimental points are from Refs. 13, 19, and 20.

ergies. The root-mean-square percentage error Δ over this range of energies is 1.5%. A slightly better fit can be obtained if Z is allowed to vary along with a and n , with the results $Z = 0.992$, $a = 0.653$, $n = 3.61$, and $\Delta = 1.2\%$. The fitted value of Z is very close to the expected value of 1. Since the experimental uncertainty of the low-energy points is $\sim 3\%$, the 1% difference is clearly not significant.

It should be noted that the values of a and n are also close to the values of ~ 1 and ~ 4 as is expected. While it is gratifying that these values are so close to the expected values, the extremely good agreement is fortuitous since the arguments given earlier for the expected magnitudes of a and n are relatively crude.

With the determined values of a , n , and Z , the formula given in Eq. (12) is clearly better, overall, than any other single approach. It should be pointed out that the Bethe-Bloch theory is meant to be applied only in the high-velocity regime, while the curves LSS, F, and BH are only meant to be applied below about 0.025 MeV. Further, the curves LSS and F have been calculated using a Thomas-Fermi model of the atom, and would not necessarily be expected to be extremely accurate for the case presented in Fig. 2. The curve labeled BH has been determined by using the method of Bhalla *et al.*⁹ with the hydrogen 1s electron wave function. A minimum impact parameter of zero was assumed however, while Bhalla *et al.* suggested that the minimum impact parameter might be ~ 1 Å. Increasing the minimum impact parameter would bring BH into better

agreement with experiment below 0.025 MeV.

The formula [Eq. (12)] thus accurately gives the stopping cross section for this case in all three velocity regimes, and over-all does so more accurately than any of the individual regime formulas. In addition, this case allows a determination of the parameter Z from first principles, confirming that such determinations are indeed possible.

In Fig. 3 similar results and comparisons are shown for helium incident on helium gas. The theoretical curves are labeled as in Fig. 2, and the experimental data are from Weyl²¹ and Chu and Powers.²² Also included in the determination of the curve BR was a theoretical point at $E = 40$ MeV taken from the tabulation of Barkas and Berger.⁵ The values of the three parameters for curve BR are $a = 0.378$, $n = 3.63$, $Z = 1.43$, and $\Delta = 1.4\%$. The remarks made concerning the theoretical curves in Fig. 2 also apply here. Once again it is clear that the formula presented in Eq. (12) gives the best over-all description of S_e . Also we again have an opportunity to check whether Z can be determined from first-principles calculations.

In order to make such a check the 1s electronic wave function for the helium atom is required. A first approximation to the wave function is the one-parameter variational wave function,²³ but a two-parameter wave function²⁴ and wave functions involving the interelectronic distance²⁵ give an increasingly accurate description of the actual wave function. The one-parameter wave function has $Z = 1.69$ which is 18% larger than the value 1.43 determined by a fit to experiment. The two-param-

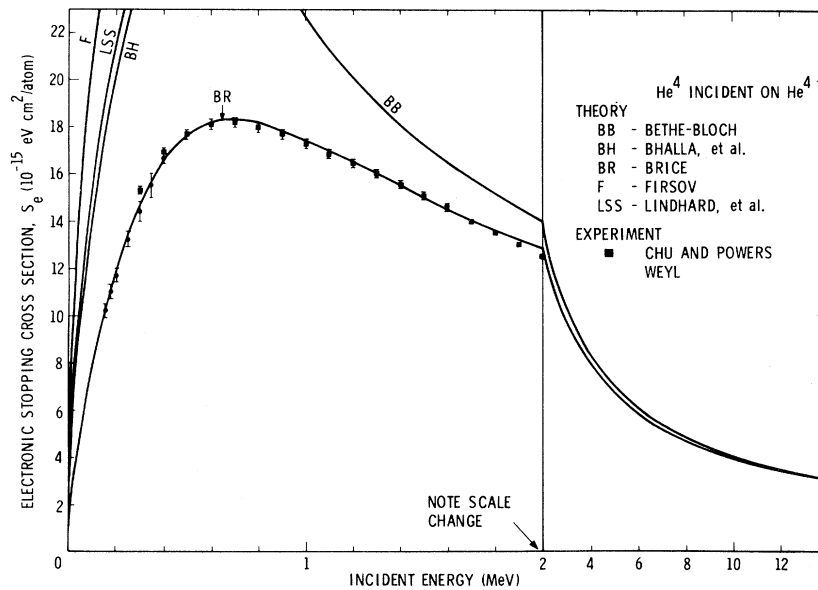


FIG. 3. Electronic stopping cross section vs incident energy for helium incident on helium. The theoretical curves shown are from the present calculation and Refs. 5-7 and 9. The experimental points are from Refs. 21 and 22.

eter wave function has two values of Z , $Z' = 1.19$ and $Z'' = 2.19$. When these are averaged, by averaging $1/Z$ in keeping with Eq. (13), one obtains $Z = 1.54$, which is only 8% greater than the fitted value. An evaluation of Z from the more complex wave functions is beyond the scope of this paper, however, it is felt that the trend to increased accuracy in Z with improved wave functions indicates that accurate determinations of Z are possible.

The formula given in Eq. (12) also gives results of comparable accuracy when fitted to the experimental data for the other $1s$ electron atom projectile and target combinations. For hydrogen incident on helium one obtains $a = 0.532$, $n = 3.55$, $Z = 1.46$, and $\Delta = 1.8\%$. For helium incident on $\frac{1}{2}H_2$ one obtains $a = 0.444$, $n = 3.67$, $Z = 1.18$, and $\Delta = 1.4\%$. The experimental data used to obtain the values of Δ were taken from Bourland *et al.*²⁶ and Reynolds *et al.*²⁰ with, in each case, a point also taken at $E/M = 10$ MeV/amu from the tabulations of Barkas and Berger.⁵

IV. RESULTS FOR OTHER PROJECTILES AND TARGETS

The stopping cross-section formula [Eq. (12)] has been derived using hydrogenic wave functions. Because of the general similarity in curves of S_e vs velocity for all projectile and target combinations it was felt to be worthwhile to determine how accurately the formula would describe S_e for collisions between atoms having other than $1s$ electrons. Quite surprisingly it has proven possible to accurately fit the formula to experimental data for any projectile-target combination that has been tried, for incident energies in the interval 0-10 MeV/amu. Comparisons between experiment and the formula are shown in Figs. 4-13 for hydrogen, helium,

and sulfur atoms incident on a variety of gaseous targets. The experimental data to which the curves were fitted are shown as the filled points, while the open points indicate other data. The data shown on the curves for incident hydrogen were taken from Barkas and Berger,⁵ Bischel,¹³ Broley and Ribe,²⁷ Chilton *et al.*,²⁸ Phillips,¹⁹ Reynolds *et al.*,²⁰ and Swint *et al.*²⁹ For incident helium the data shown are from Barkas and Berger,⁵ Bourland *et al.*,²⁶ Chu and Powers,²² and Weyl.²¹ For incident sulfur the data are all from Pierce and Blann.¹⁷ The parameters a , n , and Z , as well as the root-mean-square percentage deviation Δ between the curves and the filled points are given in Table I for incident hydrogen, in Table II for incident helium, and in Table III for incident sul-

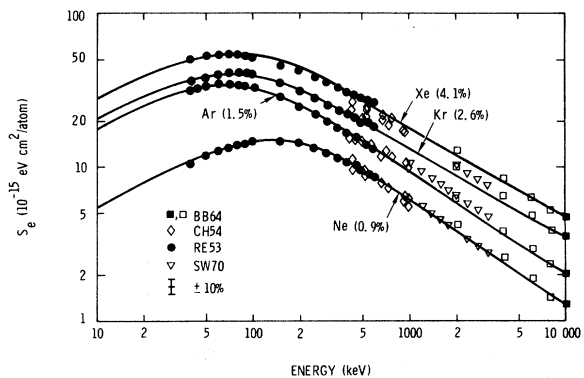


FIG. 4. Electronic stopping cross section vs incident energy for hydrogen incident on several gases. The solid curves are from Eq. (12) using the parameters listed in Table I. The data points shown are from Refs. 5, 20, 28, and 29.

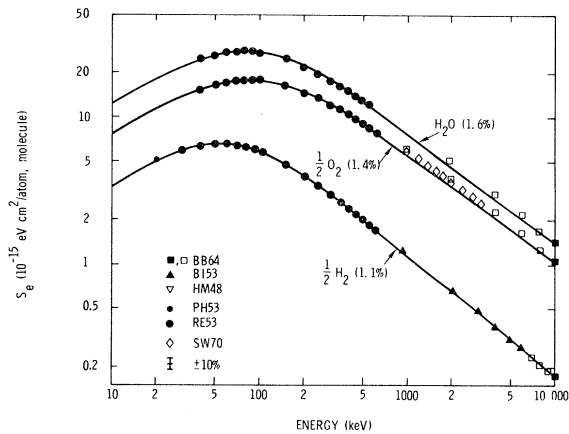


FIG. 5. Electronic stopping cross section vs incident energy for hydrogen incident on several gases. The solid curves are from Eq. (12) using the parameters listed in Table I. The data points shown are from Ref. 5, 13, 19, 20, and 29.

fur atoms.

The agreement between experiment and present theory is seen to be quite striking in all of Figs. 4-13. In several of the curves for incident hydrogen the experimental data lie ~5 to 10% above the curve in the energy region ~1 to 3 MeV/amu. These data were not used, however, in obtaining the curves, and were measured in different experimental setups from the data which were actually used to determine the parameters of the curve. The problem of deciding which data to use in determining the best fit parameters arose in several of the cases presented here, and is perhaps best illustrated for the case of hydrogen incident on xenon,

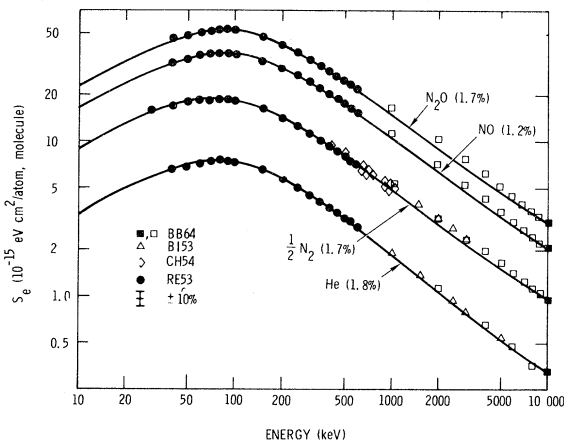


FIG. 6. Electronic stopping cross section vs incident energy for hydrogen incident on several gases. The solid curves are from Eq. (12) using the parameters listed in Table I. The data points shown are from Refs. 5, 13, 20, and 28.

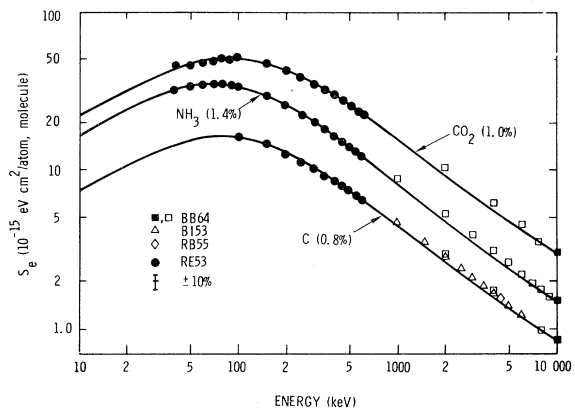


FIG. 7. Electronic stopping cross section vs incident energy for hydrogen incident on several gases. The solid curves are from Eq. (12) using the parameters listed in Table I. The data points shown are from Refs. 5, 13, 20, and 27.

Fig. 4. There, in the vicinity of 500 keV, there is an overlap of the data from Chilton *et al.*²⁸ and Reynolds *et al.*²⁰ with differences in the measured values of ~13%. In all regions, however, and for all projectile-target combinations considered here one sees that the agreement between the formula [Eq. (12)] and experiment is as good as the scatter in experimental measurements will allow.

V. DISCUSSION AND CONCLUSIONS

As mentioned earlier, the formula given here will prove useful in many respects, particularly for extrapolations to regions in which no experimental measurements have been made. The formula would be quite useful also in extrapolations from one projectile and target combination to another. This can be accomplished providing that

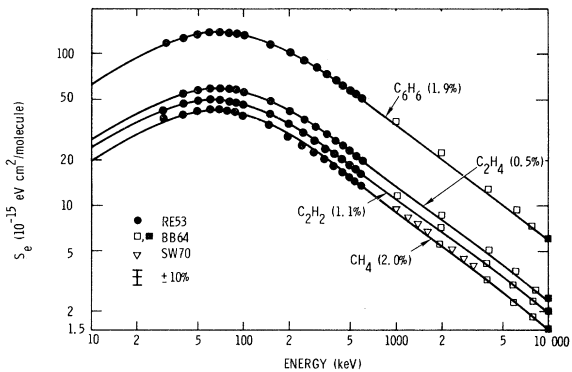


FIG. 8. Electronic stopping cross section vs incident energy for hydrogen incident on several gases. The solid curves are from Eq. (12) using the parameters listed in Table I. The data points shown are from Refs. 5, 20, and 29.

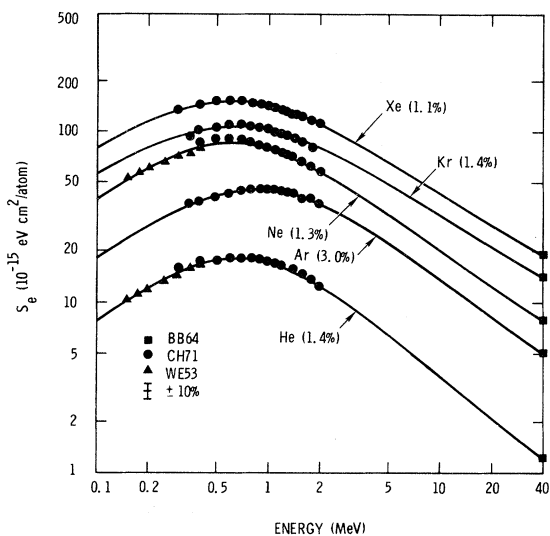


FIG. 9. Electronic stopping cross section vs incident energy for helium incident on several gases. The solid curves are from Eq. (12) using the parameters listed in Table II. The data points shown are from Refs. 5, 21, and 22.

some regular dependence of a , n , and Z on the masses (A_1, A_2) and atomic numbers (Z_1, Z_2) of the projectile and target can be established. It has already been indicated earlier that Z is calculable, in principle, from accurate atomic wave functions using the flux definition given here. It remains then to consider a and n .

The stopping cross section S_e is most sensitive to the parameters a and n at relatively high velocities. Because it enters as an exponent small changes in the parameter n can have the greatest effect on S_e . For example, at a velocity corre-

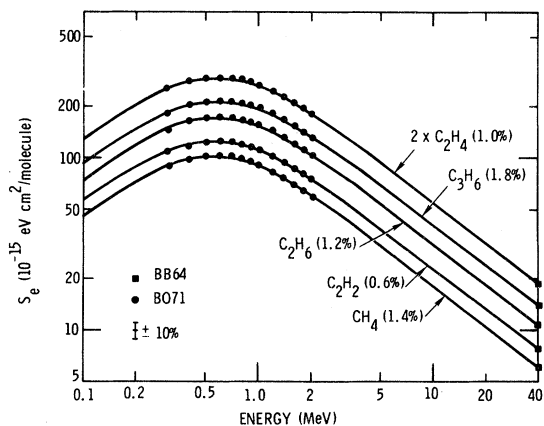


FIG. 10. Electronic stopping cross section vs incident energy for helium incident on several gases. The solid curves are from Eq. (12) using the parameters in Table II. The data points shown are from Refs. 5 and 26.

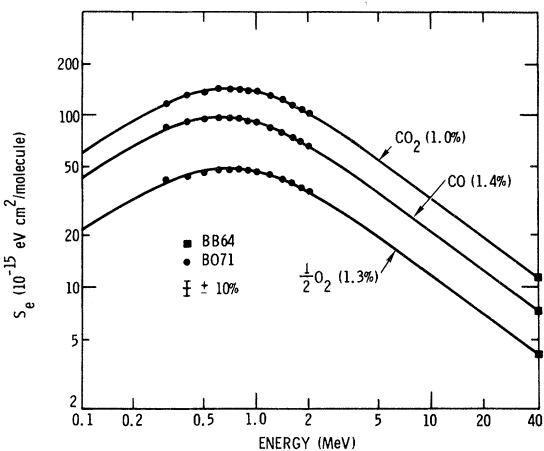


FIG. 11. Electronic stopping cross section vs incident energy for helium incident on several gases. The solid curves are from Eq. (12) using the parameters in Table II. The data points shown are from Refs. 5 and 26.

sponding to 10 MeV/amu and for the values listed in Table III, the *least* sensitive dependence of S_e on n is for sulfur incident on hydrogen. For that case a change of 0.1% in n leads to a change of 1.7% in S_e . On the other hand, a 0.1% change in the value of a at this velocity leads to a change of only 0.4% in S_e . One could not expect to extrapolate values of n with sufficient accuracy to give a good description of S_e in this velocity region, but sufficiently accurate a values might prove obtain-

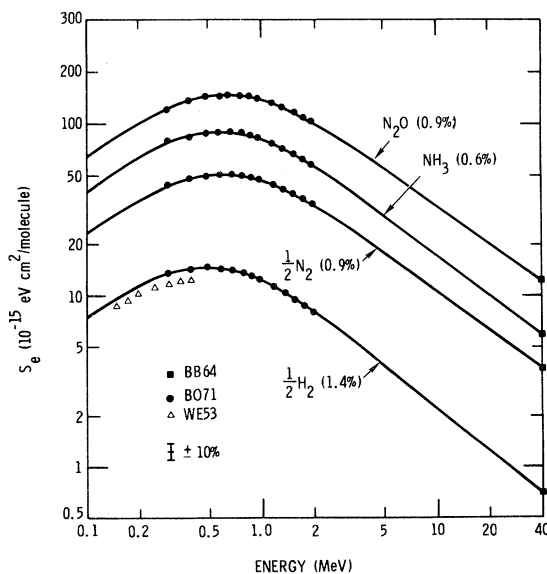


FIG. 12. Electronic stopping cross section vs incident energy for helium incident on several gases. The solid curves are from Eq. (12) using the parameters listed in Table II. The data points shown are from Refs. 5, 21, and 26.

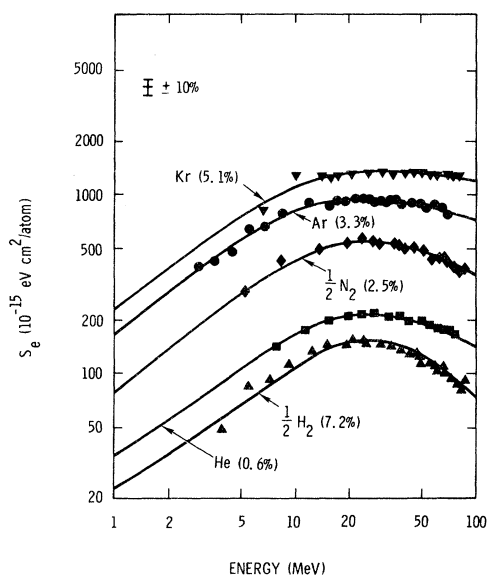


FIG. 13. Electronic stopping cross section vs incident energy for sulfur incident on several gases. The solid curves are from Eq. (12) using the parameters listed in Table III. The data points shown are from Ref. 17.

able. As it turns out, one can actually allow small errors in either a or n , and either (but not both) could be determined by extrapolation. The reason for this is that an error introduced in S_e by errors in either of the two parameters can be overcome to some extent by a compensating change in the other, but small uncorrelated errors in the param-

TABLE I. Electronic stopping cross-section parameters for hydrogen incident on various gases (incident energies 0-10 MeV).

Target	Z	a	n	Error ^a (%)
$\frac{1}{2}$ H ₂	0.9924	0.6585	3.613	1.2
He	1.4596	0.5316	3.547	1.8
$\frac{1}{2}$ N ₂	1.4151	0.5652	3.427	1.7
$\frac{1}{2}$ O ₂	1.8302	0.4925	3.404	1.4
Ne	3.0862	0.3804	3.338	0.9
Ar	1.6586	0.5772	3.308	1.5
Kr	2.6815	0.5165	3.104	2.4
Xe	3.0204	0.4923	3.109	4.2
NH ₃	1.1316	0.5855	3.512	1.4
NO	1.5656	0.5164	3.445	1.2
N ₂ O	1.5334	0.5344	3.420	1.7
H ₂ O	1.4434	0.5280	3.470	1.6
CH ₄	0.9506	0.6257	3.538	2.0
C ₂ H ₂	1.0227	0.6361	3.471	1.1
C ₂ H ₄	1.0535	0.6022	3.514	0.5
C ₆ H ₆	1.1328	0.5825	3.492	1.9
CO ₂	1.6609	0.5000	3.433	1.0
C	1.5274	0.5273	3.461	0.9

^aRoot-mean-square percentage error.

TABLE II. Electronic stopping cross-section parameters for helium incident on various gases (incident energies 0-40 MeV).

Target	Z	a	n	Error ^a (%)
$\frac{1}{2}$ H ₂	1.1812	0.4441	3.668	1.4
He	1.4301	0.3779	3.631	1.4
$\frac{1}{2}$ N ₂	1.1793	0.4130	3.513	0.9
$\frac{1}{2}$ O ₂	1.3402	0.3866	3.490	1.3
He	1.7352	0.3424	3.449	1.3
Ar	1.3602	0.4108	3.411	3.0
Kr	1.7480	0.4074	3.219	1.4
Xe	1.7863	0.4097	3.243	1.1
N ₂ O	1.1492	0.4038	3.499	0.9
NH ₃	0.9836	0.4229	3.571	0.6
CO	1.1145	0.4138	3.501	1.4
CO ₂	1.1840	0.3940	3.507	1.0
CH ₄	0.8832	0.4377	3.598	1.4
C ₂ H ₂	0.9262	0.4377	3.557	0.6
C ₂ H ₄	0.9203	0.4311	3.569	1.0
C ₂ H ₆	0.8887	0.4334	3.579	1.2
C ₃ H ₆	0.9168	0.4296	3.562	1.8

^aRoot-mean-square percentage error.

eters can lead to large changes in S_e at sufficiently high velocities as indicated above. Since the cross section is most sensitive to errors in the value of n , it was decided to concentrate on searching for regularities in the a values which might be correlated with properties of the target or projectile atoms.

Referring to the discussion after Eq. (11) one sees that a depends on the collision length l and another atomic length $v_0 T$. Each of these lengths are related to the atomic "size" of both the incident ion and the target atom. Thus a correlation between a values and the atomic size of the target and projectile atoms was sought using various measures of the atomic size. Through trial and error it was found that the a values correlated well with the root-mean-square atomic radius of the target atoms, obtained as described below.

Each electronic orbital is assigned a radius r_i which corresponds to the radius of maximum radial charge density. The root-mean-square atomic

TABLE III. Electronic stopping cross-section parameters for sulfur incident on various gases (incident energies 0-100 MeV).

Target	Z	a	n	Error ^a (%)
$\frac{1}{2}$ H ₂	2.1727	0.1719	3.990	7.2
$\frac{1}{2}$ N ₂	1.0668	0.2178	3.107	2.5
He	1.6242	0.2021	3.194	0.6
Ar	0.8523	0.2584	2.747	3.3
Kr	0.9008	0.2637	2.514	5.1

^aRoot-mean-square percentage error.

TABLE IV. Values of r calculated for various targets.

Target	r (Å)	Target	r (Å)	Target	r (Å)
He	... ^a	$\frac{1}{2}$ O ₂	0.400	CO ₂	0.444
Ne	0.299	NH ₃	0.482	CH ₄	0.539
Ar	0.458	NO	0.429	C ₂ H ₂	0.543
Kr	0.427	N ₂ O	0.439	C ₂ H ₄	0.541
Xe	...	H ₂ O	0.429	C ₂ H ₆	0.540
$\frac{1}{2}$ H ₂	0.529	C	0.545	C ₂ H ₆	0.541
$\frac{1}{2}$ N ₂	0.460	CO	0.468	C ₆ H ₆	0.543

^aOne-parameter wave function, Ref. 23, gives $r = 0.313$ Å; two-parameter wave function, Ref. 24, gives $r = 0.358$ Å.

radius r is then defined as the root-mean-square average of r_i for all occupied orbitals. For compounds a value of r is assigned which is the root-mean-square average of the r values for the constituent atoms, weighted by the number of electrons on each atom. The r values so obtained are listed in Table IV. For all atoms except hydrogen and helium the values of r_i were taken from Slater's tabulation as determined through a self-consistent central-field method.³⁰ For hydrogen the value from the exact wave function was used. For helium the one-parameter wave function²³ gave a radius $r_i = 0.313$ Å, while the two-parameter function²⁴ gave 0.358 Å, a difference of 14%. Because of this, and because a central-field model is not appropriate for the helium atom,^{24,25} results for helium targets are not included in the discussion which follows.

In Fig. 14 are shown the a values plotted as a function of the target atom r values for hydrogen projectiles. The closed points refer to elemental targets while the open points refer to compound targets. With the exception of the open triangles, which refer to targets of various carbon compounds, the points are seen to fall very nearly on

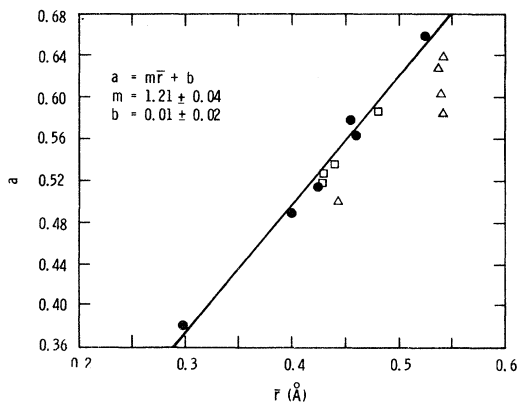


FIG. 14. Parameter a vs the target atomic radius r for hydrogen incident on various gases. Data points shown are from Tables I and IV.

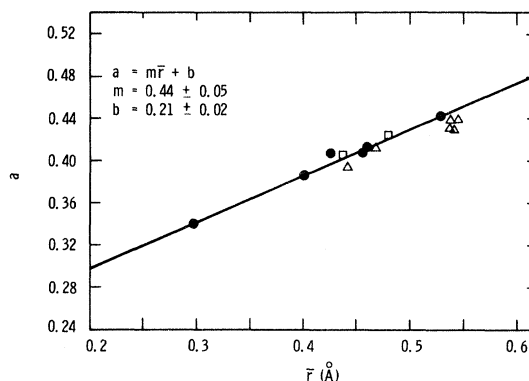


FIG. 15. Parameter a vs the target atomic radius r for incident helium. Data points shown are from Tables II and IV.

a straight line. The straight line shown in the figure was obtained by a least-mean-squares error fit to the filled points only. The slope of the line is $m = 1.21 \pm 0.04$ and its intercept is $b = 0.01 \pm 0.02$. The indicated uncertainties for m and b were obtained from the scatter of the points about the straight line. The open triangles can also be brought into good agreement with the indicated straight line if the r value for the carbon atom is reduced ~ 5 –10%. This is in agreement with the significant rearrangement which is known to occur for the carbon electrons when the atom is bound into a compound.

Similar results are shown in Figs. 15 and 16 for helium and sulfur projectiles, respectively. For helium the straight line has slope $m = 0.44 \pm 0.05$ and intercept $b = 0.21 \pm 0.02$, while for sulfur these values are $m = -0.92 \pm 0.19$ and $b = 0.66 \pm 0.09$.

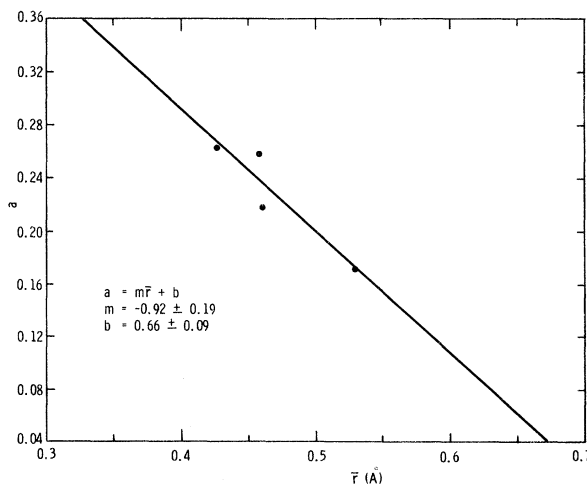


FIG. 16. Parameter a vs the target atomic radius r for sulfur incident on several gases. The data points shown are from Tables III and IV.

The general remarks given above for Fig. 14 also apply for Figs. 15 and 16. Again, in Fig. 15 it is seen that the points for the carbon-compound targets fall to the right of the straight line, although the agreement is somewhat better here than in Fig. 14. The scatter in the points in Fig. 16 probably reflects the scatter in the experimental data from which the a values were extracted (see Fig. 13).

The results shown in Figs. 14–16 indicate that a values could be extrapolated from one target to another quite easily for a fixed projectile. To obtain a values for *different* projectiles one extrapolates the values of m and b . While a simple relationship between these parameters and the values of A_1 and Z_1 is not evident from the three values quoted here for hydrogen, helium, and sulfur projectiles, a monotonic increase of b and a monotonic decrease of m with projectile atomic number is noted. With values of m and b for other projectiles one should be able to establish an empirical relationship from which extrapolation would prove possible.

Thus, of the three adjustable parameters of the formula given in Eq. (12), the parameter Z appears to be determinable from first-principles calculations, while it seems promising for a to be determined from the linear relationships shown above. The remaining parameters n can then be adjusted to give the best fit to high-energy values of S_e as determined from the Bethe–Bloch formula, or from experimental data. The parameter I_{adj} must be determined in order to be able to use the Bethe–Bloch formula, but the value of S_e is less sensitive to small errors in I_{adj} than the three-parameter formula is to errors in n . In addition, I_{adj} can be determined relatively accurately for any target.³¹

In summary, an analytic formula with three adjustable parameters, a , n , and Z , has been given for the electronic (inelastic) stopping cross section S_e which accurately gives S_e at all nonrelativistic velocities. The three parameters have been determined for hydrogen, helium, and sulfur atoms incident on a variety of gaseous targets. It has further been shown that the parameter Z is determinable from first-principles calculations, and that the parameter a is related in a simple

way to the “size” of the target atoms. Finally, a method of obtaining the last parameter n has been suggested which utilizes the Bethe–Bloch formula. The formula given for S_e is quite accurate for incident energies in the range 0–10 MeV/amu and should prove to be quite useful in obtaining S_e values in energy (velocity) regions for which no experimental data are available, or for projectile and target combinations for which there are no experimental data.

APPENDIX

The mathematical steps leading to Eq. (10) of the text are quite complicated and are presented here for completeness. Further, as indicated in the text, a first-principles determination of the parameter Z should be possible with accurate atomic wave functions, and the procedure for doing that will be essentially as presented in this Appendix.

It is desired to use the hydrogenic 1s wave function in Eqs. (8) and (9) and to enter the resultant flux in Eq. (5) to obtain the one-electron contribution to the inelastic energy loss, $W(b)$. This result is then to be used in Eq. (6) to obtain the one-electron contribution to S_e in the modified Firsov approach. Equation (5) gives $W(b)$ for the collision of two atoms; thus the collision of two atoms, each with a single 1s electron, is considered here. To obtain the *one*-electron contribution to $W(b)$ and S_e one then needs to divide the results obtained in this procedure by 2.

The 1s hydrogenic wave function is given by $\psi(\vec{\rho})$ with

$$\psi(\vec{\rho}) = \pi^{-1/2} \lambda^{3/2} e^{-\lambda \rho}. \quad (\text{A1})$$

The constant λ appearing in (A1) is given by Z/a_0 , where a_0 is the Bohr radius and Z is the nuclear charge. Taking the Fourier transform of ψ as indicated in Eq. (7a) of the text, one obtains the function $\varphi(\vec{k})$ and

$$\varphi(\vec{k}) = 2^{3/2} \lambda^{5/2} \pi^{-1} (k^2 + \lambda^2)^{-2}. \quad (\text{A2})$$

Before these specific functions are used, however, a general expression for S_e' will be derived. Entering Eq. (8) of the text into Eq. (9) one obtains the following expression for the flux Φ :

$$\Phi = \int \left[\left(\frac{\hbar}{16m\pi^3} \right) \int_{-\infty}^{\infty} dk_x \int_{-\infty}^{\infty} dk_x' \int_{-\infty}^{\infty} dk_y \int_{-\infty}^{\infty} dk_y' \int_{k_0}^{\infty} dk_z \int_{k_0}^{\infty} dk_z' (k_z + k_z' - 2k_0) e^{i(\vec{k}-\vec{k}') \cdot \vec{\rho}} \varphi(\vec{k}) \varphi^*(\vec{k}') \right] dA. \quad (\text{A3})$$

As indicated in the text the z axis is perpendicular to the Firsov plane (see Fig. 1) and thus in Eq. (A3), $dA = dx dy$. The coordinate system thus defined is not fixed, relative to atom A , but rotates as the collision between the two atoms pro-

ceeds. In the development that follows, this rotary motion will be neglected since it leads to a non-physical singularity at small impact parameters. As an argument for doing this one should note that the Firsov plane is an artifice of the calculational

procedure, and in the same spirit, the neglect of the rotary motion of the coordinate system could be regarded as a further artifice of the method.

Continuing on this basis then, at any given point the plane is effectively moving in the z direction at a velocity $w_z = dz/dt$. Thus $k_0 (= mw_z/\hbar)$ is not a function of location on the Firsov plane and the x and y integrations of Eq. (A3) can be carried out formally. For the x integration one obtains

$$\int_{-\infty}^{\infty} e^{i\Delta k_x x} dx = 2\pi\delta(\Delta k_x), \quad (\text{A4})$$

where $\Delta k_x = k_x - k'_x$ and δ is the Dirac δ function. A similar result holds for the y integration. After the x and y integration have been performed the integrations over k'_x and k'_y can also be formally completed with the net result that Eq. (A3) becomes

$$\Phi = \left(\frac{\hbar}{4\pi m}\right) \int_{-\infty}^{\infty} dk_x \int_{-\infty}^{\infty} dk_y \int_{k_0}^{\infty} dk_z \int_{k_0}^{\infty} dk'_z \\ \times e^{i(k_z - k'_z)z} (k_z + k'_z - 2k_0) \varphi(\vec{k}) \varphi^*(\vec{k}'). \quad (\text{A5})$$

One should note that the x and y components of \vec{k} and \vec{k}' are the same in (A5).

Attention is now directed to the k_z and k'_z integrations and Φ_z is defined as

$$\Phi_z = \int_{k_0}^{\infty} dk_z \int_{k_0}^{\infty} dk'_z e^{iKz} (k_z + k'_z - 2k_0) \varphi(\vec{k}) \varphi^*(\vec{k}'), \quad (\text{A6})$$

where $K = k_z - k'_z$. Introducing $q_z = k_z - k_0$ and $q'_z = k'_z - k_0$ and noting that $K = q_z - q'_z$, (A6) becomes

$$\Phi_z = \int_0^{\infty} dq_z \int_0^{\infty} dq'_z e^{iKz} (q_z + q'_z) \varphi(q_z + k_0) \varphi^*(q'_z + k_0), \quad (\text{A7})$$

where the dependence of φ and φ^* on k_x and k_y has been suppressed in the notation. The product $\varphi\varphi^*$ can now be expanded in a Taylor series as

$$\varphi(q_z + k_0) \varphi^*(q'_z + k_0) = \sum_p \frac{k_0^p}{p!} D^p [\varphi(q_z) \varphi^*(q'_z)], \quad (\text{A8})$$

where D is the differential operator

$$D = \left(\frac{\partial}{\partial q_z} + \frac{\partial}{\partial q'_z}\right) = 2 \frac{\partial}{\partial K'}. \quad (\text{A9})$$

The variable K' introduced in the second equality of (A9) is defined as $K' = q_z + q'_z$.

Changing to the variables K and K' , and utilizing (A8) and (A9), (A7) becomes

$$\Phi_z = \sum_p \frac{k_0^p 2^{p-1}}{p!} \int_0^{\infty} K' dK' \int_{-K'}^{\infty} dK \\ \times e^{iKz} \frac{\partial^p}{\partial K'^p} \left[\varphi\left(\frac{1}{2}K + \frac{1}{2}K'\right) \varphi^*\left(\frac{1}{2}K' - \frac{1}{2}K\right) \right]. \quad (\text{A10})$$

Now, from Eqs. (5) and (6) of the text

$$S_e = -2\pi mu \int_0^{\infty} b db \int_{-\infty}^{\infty} dx' \Phi, \quad (\text{A11})$$

which becomes, using (A5) and (A6) and interchanging the order of integration,

$$S_e = -\frac{1}{2} \hbar u \int_{-\infty}^{\infty} dk_x \int_{-\infty}^{\infty} dk_y \int_0^{\infty} b db \int_{-\infty}^{\infty} dx' \Phi_z. \quad (\text{A12})$$

Let S_z be defined by

$$S_z = \int_0^{\infty} b db \int dx' \Phi_z. \quad (\text{A13})$$

Substituting (A10) into (A13) and interchanging the order of integration then gives

$$S_z = \sum_p \frac{2^{p-1}}{p!} \int_0^{\infty} K' dK' \int_{-K'}^{K'} dK \frac{\partial^p}{\partial K'^p} \left[\varphi\left(\frac{1}{2}K' + \frac{1}{2}K\right) \right] \\ \times \varphi^*\left(\frac{1}{2}K' - \frac{1}{2}K\right) \int_0^{\infty} b db \int_{-\infty}^{\infty} k_0^p e^{iKz} dx'. \quad (\text{A14})$$

From Fig. 1, the coordinate x' is recognized as the negative of this projection of \vec{R} onto the original direction of motion of atom A . Thus, $4z^2 = R^2 = b^2 + (x')^2$, and it is noted that z is a positive even function of x' . The expression for k_0 then becomes

$$k_0 = \frac{m dz}{\hbar dt} = \frac{mx' dx'}{4\hbar z dt} = \frac{mx'u}{4\hbar z}, \quad (\text{A15})$$

and it is noted that k_0 is an odd function of x' .

This being the case, in (A14) the integration over x' will give zero for odd p and the equation can be rewritten as

$$S_z = 4 \sum_n \frac{(mu/2\hbar)^{2n}}{(2n)!} \int_0^{\infty} K' dK' \int_{-K'}^{K'} dK \frac{\partial^{2n}}{\partial K'^{2n}} (\varphi\varphi^*) \\ \times \int_0^{\infty} b db \int_{b/2}^{\infty} \frac{e^{iKz} (4z^2 - b^2)^{n-1/2} dz}{z^{2n-1}}. \quad (\text{A16})$$

The integrals over b and z can now be interchanged and evaluated to yield

$$S_z = -8\pi \sum_n \frac{(mu/\hbar)^{2n}}{(2n+1)!} \int_0^{\infty} K' dK' \int_{-K'}^{K'} dK \frac{\partial^{2n}}{\partial K'^{2n}} (\varphi\varphi^*) \\ \times \frac{\partial^2}{\partial K^2} \delta(K), \quad (\text{A17})$$

where $\delta(K)$ is the Dirac δ function.

If the product $\varphi\varphi^*$ is finite at $K=0$, and has finite derivatives there [conditions satisfied by the function (A2)], then the second derivative with respect to K can be transferred from the δ function to the other factor in the second integrand. The indicated integration can then be performed yielding

$$S_z = -8\pi \sum_n \frac{(mu/\hbar)^{2n}}{(2n+1)!} \\ \times \int_0^{\infty} K' \frac{\partial^{2n}}{\partial K'^{2n}} \left(\frac{\partial^2 |\varphi|^2}{\partial K'^2} \Big|_{K=0} - 4 \left| \frac{\partial \varphi}{\partial K'} \right|^2 \Big|_{K=0} \right) dK', \quad (\text{A18})$$

where it has been noted that for the arguments indicated in (A10),

$$\frac{\partial \varphi}{\partial K'} = \frac{\partial \varphi}{\partial K} \quad \text{and} \quad \frac{\partial \varphi^*}{\partial K'} = -\frac{\partial \varphi^*}{\partial K}.$$

Noting now that at $K=0$, $\frac{1}{2}K'$ is the third argument of both φ and φ^* , a change of variables to $k_z = \frac{1}{2}K'$ then yields

$$S_z = -8\pi \sum \frac{(mu/2\hbar)^{2n}}{(2n+1)!}$$

$$\times \int_0^\infty k_z \frac{\partial^{2n}}{\partial k_z^{2n}} \left(\frac{\partial^2}{\partial k_z^2} |\varphi|^2 - 4 \left| \frac{\partial \varphi}{\partial k_z} \right|^2 \right)_{k_z=0} dk_z. \quad (\text{A19})$$

The arguments of both φ and φ^* in (A19) are k_x , k_y , and k_z . Substituting this expression into (A12) and dividing by two to obtain the one-electron contribution to S_e yields after some simplification

$$S'_e = \frac{1}{2}S_e = 2\pi\hbar u \left[\int_{-\infty}^\infty dk_x \int_{-\infty}^\infty dk_y \left(|\varphi|_{k_z=0}^2 - 4 \int_0^\infty k_z \left| \frac{\partial \varphi}{\partial k_z} \right|^2 dk_z \right) \right] + 2\pi\hbar u \sum_{n=1}^\infty \frac{(mu/2\hbar)^{2n}}{(2n+1)!} \left[\int_{-\infty}^\infty dk_x \int_{-\infty}^\infty dk_y \frac{\partial^{2n-2}}{\partial k_z^{2n-2}} \left(\frac{\partial^2}{\partial k_z^2} |\varphi|^2 - 4 \left| \frac{\partial \varphi}{\partial k_z} \right|^2 \right) \right]_{k_z=0}. \quad (\text{A20})$$

It is reiterated that the expression in (A20) is general and does not depend on the $1s$ character of the wave functions. It is the first term of this expression which could be used with actual one-electron atomic wave functions for a first-principles calculation of Z . When the $1s$ wave functions from (A2) are entered in Eq. (A20) one obtains

$$S'_e = \frac{32\hbar^2}{5m} \epsilon^{1/2} \left(1 + \sum \frac{(-1)^{n+1}(2n+3)(n+2)(n+1)n\epsilon^n}{3(2n+1)(2n)(2n-1)} \right), \quad (\text{A21})$$

where $\epsilon = (mu/2\hbar\lambda)^2 = (u/2Zv_0)^2$.

For $\epsilon < 1$ the sum in (A21) converges and an

analytic form can be obtained with the aid of formula (1.517), first equation, from the tables by Gradshteyn and Ryzhik.³² The resultant formula is

$$S'_e = \frac{4\hbar^2}{5m} \left[\epsilon^{1/2} \left(\frac{30\epsilon^3 + 83\epsilon^2 + 74\epsilon + 21}{3(1+\epsilon)^3} \right) + (10\epsilon + 1) \arctan \epsilon^{1/2} \right]. \quad (\text{A22})$$

This form for S'_e has been obtained for $\epsilon < 1$. The evaluation of S'_e is extremely difficult if one does not make the series expansion (A8) and it is assumed therefore that the form (A22) is correct also for $\epsilon > 1$.

*Work supported by the U. S. Atomic Energy Commission.

¹A brief report of this work has previously been given by D. K. Brice, *Bull. Am. Phys. Soc.* **17**, 131 (1972).

²For a more complete discussion of the current status of the theory of stopping powers, see *Studies in Penetration of Charged Particles in Matter*, Natl. Acad. Sci.—Natl. Res. Council Publ. No. 1133 (Natl. Acad. Sci.—Natl. Res. Council, Washington, D. C., 1964).

³H. Bethe, *Ann. Physik* **5**, 325 (1930); F. Bloch, *ibid.* **5**, 285 (1933).

⁴U. Fano, *Ann. Rev. Nucl. Sci.* **13**, 1 (1963), reprinted as Appendix A in Ref. 2.

⁵W. H. Barkas and M. J. Berger, in Ref. 2, p. 103.

⁶J. Lindhard, M. Scharff, and H. E. Schiott, *Kgl. Danske Videnskab. Selskab, Mat.-Fys. Medd.* **33**, No. 14 (1963); J. Lindhard and M. Scharff, *Phys. Rev.* **124**, 128 (1961).

⁷O. B. Firsov, *Zh. Eksperim. i Teor. Fiz.* **36**, 1517 (1959) [*Sov. Phys. JETP* **36**, 1076 (1959)].

⁸Ya. A. Teplova, V. S. Nikolaev, I. S. Dmitriev, and L. N. Fateeva, *Zh. Eksperim. i Teor. Fiz.* **42**, 44 (1962) [*Sov. Phys. JETP* **15**, 31 (1962)].

⁹C. P. Bhalla, J. N. Bradford, and G. Reese, *Atomic Collision Phenomena in Solids*, edited by D. W. Palmer, M. W. Thompson, and P. D. Townsend (North-Holland, Amsterdam, 1970), p. 361.

¹⁰J. M. Cheshire, G. Dearnaley, and J. M. Poate,

Phys. Letters **27A**, 318 (1968).

¹¹W. D. Wilson, R. D. Hatcher, and C. L. Bisson, *Bull. Am. Phys. Soc.* **16**, 333 (1971).

¹²J. O. Hirshfelder and J. L. Magee, *Phys. Rev.* **73**, 207 (1948); **79**, 1005 (1950).

¹³H. Bischel, in *Handbook of Physics*, (McGraw-Hill, New York, 1963), Sec. 8c; M. C. Walske, *Phys. Rev.* **88**, 1283 (1952); **101**, 940 (1956).

¹⁴L. C. Northcliffe and R. F. Schilling, *Nucl. Data, Sec. A* **7**, 4 (1970); see also L. C. Northcliffe, *Ann. Rev. Nucl. Sci.* **13**, 67 (1963), reprinted as Appendix B of Ref. 2.

¹⁵A phenomenological theory of the inelastic energy loss in a single collision of neutral atoms which is apparently valid for the intermediate- or high-velocity regimes has been given by A. Russek and M. T. Thomas, *Phys. Rev.* **109**, 2015 (1958).

¹⁶See J. H. Ormrod and H. E. Duckworth, *Can. J. Phys.* **41**, 1424 (1963); J. H. Ormrod, J. R. MacDonald, and H. E. Duckworth, *ibid.* **43**, 275 (1965).

¹⁷T. E. Pierce and Marshall Blann, *Phys. Rev.* **173**, 390 (1968).

¹⁸The expression for S'_e depends linearly on the projectile velocity at low velocities, in agreement with previous low-velocity theories (see, e.g., Refs. 6–11). At high velocities S'_e varies quadratically with the velocity, in agreement with the high-velocity dependence which would be predicted by the energy-loss formula of Ref. 15.

- ¹⁹J. A. Phillips, Phys. Rev. **90**, 532 (1953).
²⁰H. K. Reynolds, D. N. F. Dunbar, W. A. Wenzel, and W. Whaling, Phys. Rev. **92**, 742 (1953).
²¹Peter K. Weyl, Phys. Rev. **91**, 289 (1953).
²²W. K. Chu and D. Powers, Phys. Rev. B **4**, 10 (1971).
²³See, Leonard I. Schiff, *Quantum Mechanics*, 2nd ed. (McGraw-Hill, New York, 1955), p. 174.
²⁴R. G. Taylor and R. G. Parr, Proc. Natl. Acad. Sci. U. S. **38**, 154 (1952).
²⁵See, e.g., E. A. Hylleraas, Z. Physik **54**, 347 (1939); C. L. Pekeris, Phys. Rev. **122**, 1649 (1958).
²⁶P. D. Bourland, W. K. Chu, and D. Powers, Phys. Rev. B **3**, 3625 (1971).
²⁷J. E. Brolley, Jr. and F. L. Ribe, Phys. Rev. **98**, 1112 (1955).
²⁸Arthur B. Chilton, John N. Cooper, and James C. Harris, Phys. Rev. **93**, 413 (1954).
²⁹J. B. Swint, R. M. Prior, and J. J. Ramirez, Nucl. Instr. Methods **80**, 134 (1970).
³⁰J. C. Slater, *Quantum Theory of Atomic Structure*, (McGraw-Hill, New York, 1960), Vol. 1, p. 210.
³¹J. E. Turner, Ref. 2, p. 99.
³²I. S. Gradshteyn and I. M. Ryzhik, *Table of Integrals, Series, and Products*. (Academic, New York, 1965).
 Note that the quoted formula is incorrect in this tabulation. The argument of the arctangent should be $x^{1/2}$.

PHYSICAL REVIEW A

VOLUME 6, NUMBER 5

NOVEMBER 1972

Energy Distribution of Electrons Produced in Low-Velocity Ionizing Collisions of Argon Atoms

H. W. Berry

Physics Department, Syracuse University, Syracuse, New York 13210

(Received 7 July 1972)

The energy distribution of electrons has been measured for ionizing collisions of Ar with Ar in the center-of-mass energy range of 30–250 eV. The distributions display several prominent peaks which can be attributed to the autoionization of highly excited atomic and molecular states.

The study of the energies of electrons ejected in ionizing collisions of ion and atoms at rest has shown that these electrons are ejected with both discrete and continuous energy distributions.^{1–5} In many cases the definite energies have been correlated with autoionizing states of one of the particles in the collision. The work reported here extends the measurements for the Ar-Ar system to low-collision energies that range from 30 to 250 eV in the center-of-mass system. Particularly, for ionizing collisions of neutral Ar with Ar, the ejected-electron distributions show a spectrum dominated by a number of discrete groups with a surprisingly low continuous background.

APPARATUS

The experimental method^{1,2} consisted, in brief, of producing an ion beam of the desired energy, in collimating the beam with an appropriate lens system, and of neutralizing the beam by charge exchange. The collision region in which the ionization occurs was surrounded by a fine wire grid to suppress the electron ejection produced by ion or atom bombardment of the walls. Ionization electrons ejected at right angles to the beam from a region in the center of the grid were selected by a 90° cylindrical electrostatic energy analyzer and were counted in a system containing a continuous-dynode secondary-electron multiplier followed by a pulse amplifier and a counting circuit. Back-

ground counting rates of this multiplier were as low as several per minute, thus allowing valid measurements of 20 per minute, which was the average value for the 30-eV collision. The energy spread of the beam was about 2 eV full width at half-maximum for the 100-eV beam. This would be about the same for the neutral atom beam, since the maximum allowable angle of scattering in a neutralizing collision was about 1°.

The electrostatic analyzer had an effective slit width proportional to the energy selected. However, by use of an accelerating system between the ionizing region and the analyzer, the electron-energy range was held to about one-half of the maximum energy observed. In the data shown, no correction was made for the variable slit width. The resolution of the analyzing system is indicated by the sharp rise at the zero of the intrinsic electron energy. The major part of this rise occurred in about 0.2 eV, except for the lowest collision energies, where the count rate was so low that a long-time-constant circuit was needed. This circuit behavior was largely responsible for the broad peaks in the 30-eV collision spectrum.

The gas pressure at the point of the ionizing collision was determined from the fraction of the ion beam neutralized per unit path. Similarly, the size of the neutral beam was determined from the loss in the ion beam with gas present in the neutralizing region and from the geometrical fac-